Lysine-69 Plays a Key Role in Catalysis by Ornithine Decarboxylase through Acceleration of the Schiff Base Formation, Decarboxylation, and Product Release Steps†

Andrei L.Osterman,‡ Harold B. Brooks,§ Laurie Jackson, Jared J. Abbott, and Margaret A. Phillips*

Department of Pharmacology, The University of Texas Southwestern Medical Center at Dallas, 5323 Harry Hines Blvd, Dallas, Texas 75235-9041

Received March 18, 1999; Revised Manuscript Received May 28, 1999

ABSTRACT: Ornithine decarboxylase (ODC) is a pyridoxal-5′-phosphate-dependent (PLP) enzyme that catalyzes the biosynthesis of the polyamine putrescine. Similar to other PLP-dependent enzymes, an active site Lys residue forms a Schiff base with PLP in the absence of substrate. The mechanistic role of this residue (Lys-69) in catalysis by *Trypanosoma brucei* ODC has been studied by analysis of the mutant enzymes, in which Lys-69 has been replaced by Arg (K69R ODC) and Ala (K69A ODC). Analysis of K69A ODC demonstrated that the enzyme copurified with amines (e.g. putrescine) that were tightly bound to the active site through a Schiff base with PLP. In contrast, on the basis of an absorption spectrum of K69R ODC, PLP is likely to be bound to this mutant enzyme in the aldehyde form. Pre-steady-state kinetic analysis of the reaction of K69R ODC with L-Orn and putrescine demonstrated that the rates of both the product release ($k_{off.Put} = 0.0041$ s^{-1}) and the decarboxylation ($k_{decarb} = 0.016$ s^{-1}) steps were decreased by10^4-fold in comparison to wild-type ODC. Further, the rates of Schiff base formation between K69R ODC and either substrate or product have decreased by at least 10^3-fold. Product release remains as the dominant rate-limiting step in the reaction (the steady-state parameters for K69R ODC are $k_{cat} = 0.0031$ s^{-1} and $K_m = 0.18$ mM). The effect of mutating Lys-69 on the decarboxylation step suggests that Lys-69 may play a role in the proper positioning of the α-carboxylate for efficient decarboxylation. K69R ODC binds diamines and amino acids with higher affinity than the wild-type enzyme; however, Lys-69 does not mediate substrate specificity. Wild-type and K69R ODC have similar ligand specificity preferring to bind putrescine over longer and shorter diamines. Kinetic analysis of the binding of a series of diamines and amino acids to K69R ODC suggests that noncovalent interactions in the active site of K69R ODC promote selective ligand binding during Schiff base formation.

Ornithine decarboxylase (ODC)[1] is a pyridoxal-5′-phosphate (PLP)-dependent enzyme that catalyzes the decarboxylation of L-Orn to produce putrescine. This reaction is the rate-limiting step in the biosynthesis of polyamines (putrescine, spermidine, and spermine), which are required for cell growth and differentiation (*1*). Inhibitors of ODC have been utilized in the treatment of a number of proliferative diseases, including pneumocystis pneumonia and cancer (*2*, *3*). The most successful application of these inhibitors has been for the treatment of African sleeping sickness, caused by the parasitic protozoa *Trypanosoma brucei* (*4*).

The X-ray structure of mouse ODC has recently become available (*5*), and the structure confirms the prediction (*6*) that the enzyme folds into two domains, an N-terminal β/α-barrel domain and a C-terminal β-sheet domain. The PLP-binding site is largely formed within the N-terminal β/α-barrel domain, while the substrate binding site is formed in the subunit interface between the N-terminal domain of one subunit and the C-terminal domain of the other. For all characterized PLP-dependent enzymes, PLP is bound to the enzyme through a Schiff base (internal aldimine) between the carbonyl group of PLP and a Lys residue in the active site. For ODC, Lys-69 was identified by reduction and peptide mapping as the residue that forms a Schiff base with PLP (*7*). This residue typically does not play a role in high-affinity PLP binding but instead serves a number of essential catalytic functions. For aspartate aminotransferase, Lys-258 functions as a general base to catalyze α-proton abstraction (*8*, *9*) and to facilitate the formation of the Schiff base (external aldimine) with substrate (*10*). A similar result has been reported for the role of Lys-145 in D-amino acid

† This work was supported by grants (to M.A.P.) from the National Institute of Health (R01 AI34432), the Welch Foundation (I-1257), and the American Heart Association and grants (to H.B.B.) from the National Institutes of Health (F32 AI09495).

* To whom all correspondence should be addressed. Tel: (214) 648-3637. Fax: (214) 648-9961. E-mail: philli01@utsw.swmed.edu.

‡ Present address: Integrated Genomics Inc., 2201 W. Campbell Park Dr., Chicago, IL 60612.

§ Present address: Eli Lilly Co., Lilly Corporate Center, Indianapolis, IN 46285.

[1] Abbreviations: ODC, *Trypanosoma brucei* ornithine decarboxylase; mutant enzymes abbreviated by their single letter code, e.g. K69R ODC, Lys-69 to Arg mutant of ODC; PLP, pyridoxal-5′-phosphate.

10.1021/bi9906221 CCC: $18.00
Published on Web 08/19/1999

transferase (*11*, *12*). Likewise, for tryptophan synthase, Lys-87 has been demonstrated to accelerate the rates of Schiff base formation and decay and the rates of the catalytic step, including proton abstraction and β-elimination of the serine hydroxyl (*13*). For alanine racemase, Lys-39 has been demonstrated to function as the catalytic base (*14*).

Although the catalytic role of Lys has been studied in other PLP-dependent enzymes, the role of the Lys residue has not been extensively studied for any of the PLP-dependent decarboxylases. For these enzymes, decarboxylation of the α-CO_2 replaces the proton abstraction step. Thus, there is no role for a general base in this step of the reaction. None-the-less the Lys residue has been demonstrated to be essential for the activity of both, histidine decarboxylase (*15*) and ODC (*16*, *17*). Despite these studies it remains unclear what functional role Lys-69 plays in the catalytic cycle. The reaction mechanism for wild-type ODC has been previously studied by stopped-flow spectroscopy, and product release was found to be a rate-determining step (*18*). In this paper we describe mechanistic analysis of the K69R mutant of *T. brucei* ODC by pre-steady-state kinetic analysis of substrate and product binding and of the decarboxylation step. In addition, binding analysis of a series of diaimine and amino acids was done for wild-type and K69R ODC to assess factors that contribute to substrate specificity.

EXPERIMENTAL PROCEDURES

Materials. HPLC grade acetonitrile, trifluoroacetic acid, amino acids, amines, buffers, and the PLP derivatives, pyridoximine-5′-phosphate and 4-deoxypyridine-5′phosphate, were purchased from Sigma. Ni^{2+}−agarose was purchased from Qiagen. Centricon concentrators were purchased from Amicon.

Methods. Site-Directed Mutagenesis, ODC Expression, and Purification. The construction of clones encoding K69A *T. brucei* ODC has been previously described (*19*). The clone encoding K69R *T. brucei* ODC was generated by standard Kunkel mutagenesis (*20*) using the oligo 5′-CCGTTTTACGCcGT*ACG*ATGCAACGATG-3′ to substitute the codon for Arg (italicized) at position 69 and introduce a silent Spl I site (small letter). Wild-type and mutant ODCs were expressed from the cloned gene as a His-tag fusion protein in BL21/DE3 cells, from the T7 promoter as described (*19*). The enzyme was purified by Ni^{2+}−agarose column chromatography and gel filtration as previously described (*18*, *21*). ODC was concentrated to 1 mM in the presence of 2 mM PLP and 5 mM DTT. The excess of both reagents was removed using Fast Desalting HR 10/10 column (Pharmacia), equilibrated with 20 mM Hepes−NaOH pH 7.2, 50 mM NaCl, and aliquots were stored at −80 °C. The protein concentration in all ODC samples was determined by absorbance spectroscopy using a previously determined extinction coefficient of $\epsilon = 0.85$ OD $(mg/mL)^{-1}$ cm^{-1} (*19*).

Chemical Analysis of the PLP-Cofactor in K69A and Wild-Type ODC. $NaBH_4$ Reduction of Enzyme-Bound PLP. Samples of K69A and wild-type ODC were treated with $NaBH_4$ (10 mg/mL added dry directly to samples) for 2 h on ice, followed by overnight dialysis in native (buffer A: 20 mM Hepes pH 7.5, 50 mM NaCl, 1 mM DTT) or denaturing conditions (buffer A plus 8 M urea). Absorption spectra (300−500 nm) were recorded before and after reduction and dialysis to probe for the presence of PLP.

Chromatographic Analysis of Reduced PLP−External Aldimine Adducts. K69A ODC and wild-type ODC samples (0.4 mM ODC, 10 mM Hepes pH 7.5, 25 mM NaCl) were treated with $NaBH_4$ (10 mg/mL for 5 min at ambient temperature) in the presence or absence of putrescine (40 mM). Samples were brought to 7.2 M urea in 50 mM Bicine pH 9 to denature the enzyme, and the free PLP adducts were separated from ODC in a Centricon P10 concentrator. Aliquots of the flow-through were quantitatively analyzed by ion-exchange chromatography on Resource Q 5/5 column (Pharmacia) in a pH/salt gradient (buffer A, 25 mM Tris-HCl pH 9.0; buffer B, 25 mM Tris-HCl pH 7.1, 250 mM NaCl). The elution was performed at 3 mL/min, in two linear segments (0−50% B in 7 min and 50−100% B in 3 min). Retention times and molar areas were determined for a set of standards, prepared from PLP and various amines (e.g. putrescine, L-Orn, and 2-amino ethanol). Retention times range from 157 to 337 s for the reduced PLP−putrescine and for pyridoxine 5′-phosphate, respectively.

Measurement of UV−Vis Spectra and Analysis of the pH Titration of the Spectral Data. UV−vis spectra of wild-type and mutant ODCs (30 μM) were obtained as described (*22*). The minimal model that describes the spectral pH titration data for K69R ODC requires a cooperative $2H^+$ dissociation. Milimolar absorptivities observed at 335 nm (ϵ_{obs}^{335nm}) were fitted to eq 1, which describes the interconversion of the two

$$\epsilon_{obs}^{335nm} = R\left(\epsilon_{EH}^{335nm}\frac{[H^+]^2}{K_a^2 + [H^+]^2} + \epsilon_{E}^{335nm}\frac{K_a^2}{K_a^2 + [H^+]^2}\right) \quad (1)$$

spectrally distinct forms (E and EH_2), having extinction coefficients of ϵ_E^{335nm} and ϵ_{EH}^{335nm}. *R* is a correction factor and represents the molar fraction of enzyme-bound PLP, calculated as $([PLP]_{total} - [PLP]_{free})/[ODC]_{total}$. $[PLP]_{total}$ and $[PLP]_{free}$ were experimentally determined by phenylhydrazine assay in combination with ultrafiltration (*22*). For wild-type and K69R ODC, in the absence of exogenous amines, *R* is close to 1.0 at pH 6.5−7.5 but decreases to 0.6 at pH 9.5. As with wild-type ODC, no appreciable PLP dissociation was observed at pH 7.5 upon incubation of K69R ODC with L-Orn or putrescine.

Steady-State and Pre-Steady-State Measurement of K69R ODC Catalyzed Decarboxylation of L-Orn. ODC was assayed using a modified version of the $^{14}CO_2$ trapping assay (*23*). ODC (4−40 μM) was incubated with 1-[^{14}C]-L-Orn (0.03−2 mM) in 0.1 M Hepes pH 7.5, 1 mM DTT, at 37 °C in a microtube sealed into a chamber capped with a rubber septum. Whatman paper strips, soaked in saturated $Ba(OH)_2$, were inserted in the chamber prior to capping to trap released $^{14}CO_2$. The reaction was initiated by adding ODC with a microsyringe through the rubber septum (final reaction volume 0.1 mL) and stopped by addition of 40% TCA (0.2 mL). $^{14}CO_2$ trapped on the filter paper was quantitated by liquid scintillation counting. For pre-steady-state analysis, data were collected over a time range of 30−500 s. For steady-state analysis, rates were calculated after 2−15

Scheme 1

$$E + S \underset{k_{off.Orn}}{\overset{k_{on.Orn}}{\rightleftharpoons}} ES \xrightarrow{k_{decarb}} EP$$

turnovers (0.5−3 h incubation) and the data were fitted to the standard Michaelis−Menten equation to determine k_{cat} and $K_{M.}$

Single Turnover Kinetic Analysis of the Reaction of K69R ODC with L-Orn. An excess of ODC (0.1−1 mM) was incubated with minimal amounts of 1-[^{14}C]-L-Orn (0.02 mM, 56 mCi/mmol) in 0.1 M Hepes pH 7.5 at 37 °C for 30−600 s. The reaction was stopped by addition of TCA (final concentration 30%) and $NaHCO_3$ (final concentration 2.5 mM). The open tubes were incubated for 1 h in a desiccator with granulated KOH to deplete the $^{14}CO_2$ formed during the course of the reaction. The remaining counts in solution were quantitated. A 100% substrate depletion was observed in control samples (30 min reaction time).

The decay of $^{14}CO_2$ from solution under single turnover conditions (e.g. [E] ≫ [S]) follows first-order kinetics, and the data were fitted to eq 2A to obtain k_{obs} (the observed

$$[Orn] = [Orn]_0 e^{-k_{obs}t} \tag{2A}$$

first-order rate constant for the decarboxylation of L-Orn). The k_{obs} data were fitted to eq 2B (*24*), which describes a

$$k_{obs} = \frac{k_{decarb}[E]}{K_{m.decarb} + [E]} \tag{2B}$$

one-step binding model, followed by an irreversible decarboxylation step (Scheme 1), where E represents the total concentration of ODC in the reaction, ES and EP represent the Schiff base species of ODC with L-Orn and putrescine, respectively, k_{decarb} is the first-order rate constant for the chemical conversion (decarboxylation), and $K_{m.decarb}$ is the Michaelis constant for the steps up to decarboxylation.

Pre-Steady-State Kinetic Analysis of Diamine and Amino Acid Binding to K69R ODC by Single Wavelength UV−Vis Spectral Analysis. The binding of ligands (L) to K69R ODC or to free PLP was followed by spectral assay at 415 nm. Increases in absorbance at this wavelength are characteristic of Schiff base formation between the aldehyde of PLP and an amine. Briefly, enzyme (3−24 μM) or PLP (25−50 μM) was mixed with amino acid or diamine (0.006−50 mM), in 0.1 M Hepes buffer pH 7.5 at 37 °C. Absorbance readings taken at 415 nm were recorded at 0.5−20 s intervals for 30−6000 s. DTT (1 mM) was included for the analysis of the L-Orn binding reaction. In contrast to wild-type ODC (*18*), the addition of DTT does not affect the pre-steady-state kinetics of the reaction of K69R ODC with L-Orn, either when monitored by CO_2 release or by spectral analysis. However, DTT is important to stabilize the mutant enzyme over the long reaction times required to collect data.

For all ligands except L-Orn, absorbance readings at each ligand concentration were fitted to a pseudo-first-order kinetic model (eq 3A), where A_0 is the absorbance reading prior to

$$A_t = A_{eq} - \Delta A e^{-k_{obs}t} \tag{3A}$$

ligand addition, A_t is the absorbance reading at the time t,

Scheme 2

$$E + L \underset{}{\overset{K_{EL'}}{\rightleftharpoons}} [EL'] \underset{k_{-2}}{\overset{k_{+2}}{\rightleftharpoons}} EL_s$$

Scheme 3

$$E + L \underset{k_{off}}{\overset{k_{on}}{\rightleftharpoons}} EL_s$$

Scheme 4

$$E + S \underset{k_{off.Orn}}{\overset{k_{on.Orn}}{\rightleftharpoons}} ES \xrightarrow{k_{decarb}} EP \xrightarrow{k_{off.Put}} E + P$$

and A_{eq} is the absorbance reading at equilibrium. Amplitude data ($\Delta A = A_{eq} - A_0$) were fitted to eq 3B (K_d > 0.1 mM)

$$\Delta A = \Delta\epsilon_{415nm} \frac{[E][L]}{(K_d + [L])} \tag{3B}$$

$$\Delta A = \Delta\epsilon_{415nm} \frac{K_d + [L] + [E] - \sqrt{(K_d + [L] + [E])^2 - 4[E][L]}}{2} \tag{3C}$$

or to eq 3C (K_d < 0.1 mM) to determine the overall dissociation constant (K_d) for Schiff base formation between ligand (L) and K69R ODC or PLP, where E represents the total concentration of K69R ODC or free PLP.

For ligands where k_{obs} had a hyperbolic dependence on ligand concentration the k_{obs} data were fitted to eq 3D which

$$k_{obs} = k_{+2} \frac{[L]}{K_{EL'} + [L]} + k_{-2} \tag{3D}$$

describes a two-step binding model (Scheme 2), assuming a rapid equilibrium first step (*24*). $K_{EL'}$ is the dissociation constant for the intermediate formed prior to the formation of the Schiff base species, and k_{+2} and k_{-2} are first-order rate constants for the interconversion between the intermediate (EL′) and the final Schiff base species (EL_s). For ligands where the dependence of k_{obs} versus concentration was linear, the data were fitted to eq 3E, describing a single-step binding

$$k_{obs} = k_{on}[L] + k_{off} \tag{3E}$$

model (Scheme 3), to determine k_{on} and k_{off}. The parameters in eq 3D are related to those in eq 3E as follows: $k_{on} = k_{+2}/K_{EL'}$ and $k_{off} = k_{-2}$ (*24*). For ligands in which saturation of k_{obs} occurs, k_{on} and k_{off} were determined accordingly. k_{on} is the apparent second-order rate constant for the formation of the Schiff base species from free enzyme and ligand, and k_{off} is the first-order rate constant for the decay of the Schiff base species to free enzyme and ligand.

For L-Orn, at low concentrations (0.05−0.5 mM) the time-resolved absorption data were instead fitted to eq 4, which describes a three-step model (Scheme 4) that accounts for the additional component of decarboxylation on the kinetics of the observed spectral changes. Eq 4 was derived by summation of the equations describing the concentration profile of the ES (E.Orn) and EP (E.Put) species, previously reported for this model (Scheme 4) by Hiromi (*24*). For this

$$A_t = \epsilon([\text{E.Orn}] + [\text{E.Put}])_t + A_0 \quad (4)$$

$$([\text{E.Orn}] + [\text{E.Put}])_t = \frac{k_{\text{on.Orn}}[\text{Orn}][E_0]}{Q}(Me^{-Ft} + Ne^{-Gt} + k_{\text{off.Orn}} + k_{\text{off.Put}})$$

$$F = -\frac{(P - (P^2 - 4Q)^{1/2})}{2}$$

$$G = -\frac{(P + (P^2 - 4Q)^{1/2})}{2}$$

$$M = \frac{(Q - k_{\text{off.Put}}G)(k_{\text{off.Put}} + k_{\text{decarb}} - F)}{(G - F)(k_{\text{off.Put}} - F)}$$

$$P = k_{\text{on.Orn}}[\text{Orn}] + k_{\text{off.Orn}} + k_{\text{decarb}} + k_{\text{off.Put}}$$

$$Q = k_{\text{on.Orn}}[\text{Orn}](k_{\text{off.Put}} + k_{\text{decarb}}) + k_{\text{off.Put}}(k_{\text{off.Orn}} + k_{\text{decarb}})$$

$$N = \frac{(k_{\text{off.Put}}F - Q)(k_{\text{off.Put}} + k_{\text{decarb}} - G)}{(G - F)(k_{\text{off.Put}} - G)}$$

analysis the extinction coefficients for E.Orn and E.Put were assumed to be equivalent, based on the observation that the extinction coefficients of K69R ODC bound PLP are the same when bound to putrescine and D-Orn.

At high L-Orn concentration (2−25 mM) data were fitted to eqs 3A,D as described for putrescine, except that k_{-2} was neglected, based on the finding that $k_{+2.\text{Orn}}$ is sufficiently larger than k_{decarb} and $k_{\text{off.Orn}}$.

CD Analysis of External Aldimine Formation in Wild-Type and K69R ODC. The K_d for the formation of the Schiff base species between wild-type ODC and putrescine was determined by following the change in the CD spectrum at 420 nm upon ligand binding. Reactions were performed in the same conditions as described above for spectral analysis of amine binding to K69R ODC. The amplitude data were fitted to eq 5 to determine the K_d for Schiff base formation between

$$\theta_{\text{eq}} = \theta_{\text{E}}\frac{K_d}{K_d + [\text{Put}]} + \theta_{\text{EA}}\frac{[\text{Put}]}{K_d + [\text{Put}]} \quad (5)$$

putrescine and ODC, where θ_{eq} is the measured elipticity at equilibrium, θ_{E} is the elipticity measured for free ODC, and θ_{EA} is the elipticity measured at saturation (e.g. θ_{max}).

Kinetic Analysis of Arg Decarboxylation by Wild-Type ODC. Wild-type ODC (5−10 μM) was incubated with L-Arg (2.5−150 mM) in 15 mM K−phosphate buffer pH 7.4, containing 1 mM DTT and 0.15 mM PLP, at 37 °C for 1.5−18 h. The reaction was stopped by addition of TCA to 5%. Cadaverine was added as an internal standard to a final concentration of 25% of the L-Arg concentration. An aliquot (2−4 μmol) was derivatized using the AccQ·TAG kit (Waters, Milford, MA). Derivatized amino acids and diamines were analyzed by HPLC on an AccQ·TAG column using the manufacturers recommended buffers and a modified gradient (0 min, 0% B; 1 min, 5% B; 10 min, 30% B; 35 min, 100% B). The column was calibrated using standard samples (25−100 pmol) of the following amino acids derivatized as above: L-Arg (retention time (RT) = 8.4 min), agmatine (RT = 10.4 min), L-Orn (RT = 13.3 min), putrescine (RT = 19.0 min), and cadaverine (RT = 21.2 min). The concentration of agmatine in the analyzed samples was determined from a standard curve generated from known concentrations of L-Arg and agmatine, with respect to the internal standard, and the rates of L-Arg decarboxylation were calculated. Data were fitted to the standard Michaelis−Menten equation, to determine K_m and k_{cat}.

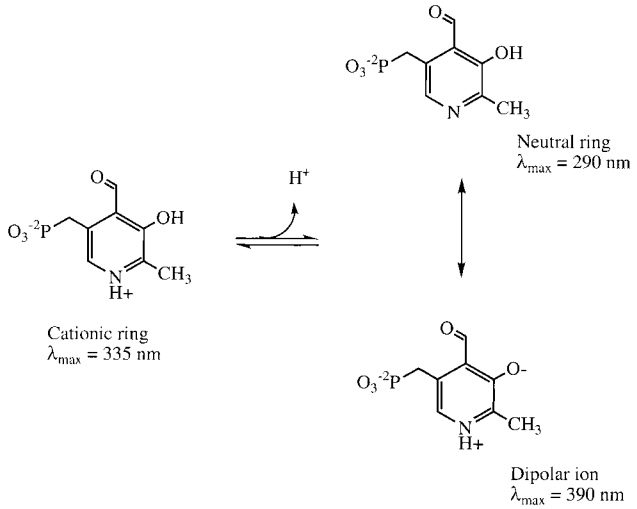

FIGURE 1: Predicted tautomers of PLP bound to K69R ODC. The spectral properties of the PLP tautomers were taken from refs *25*−*27*, where they were determined for model compounds and analysis of PLP-dependent enzymes.

Curve Fitting Analysis. All data analysis to determine model-derived kinetic parameters was performed by nonlinear curve fitting using Sigma Plot 4.0 (SPSS Inc., Chicago, IL).

RESULTS

Analysis of PLP Binding Affinity. K69A ODC and K69R ODC expressed to similar levels as the wild-type enzyme, and like wild-type ODC, they behave as dimers by gel filtration analysis. The PLP binding affinity was measured as previously described (*22*). Both mutant enzymes had similar affinity for PLP as the wild-type enzyme across the pH range from 6.5 to 9.0.

Spectral Properties of PLP Bound to the K69 Mutants of ODC. K69A vs Wild-Type ODC. Wild-type ODC displays spectral maxima at 335 and 420 nm (*22*). These spectral bands are characteristic of a Schiff base species with PLP and arise from the internal aldimine to Lys-69. The spectral properties of the PLP aldehyde are known to differ significantly from the internal aldimine and to give rise to maxima at 290, 390, and/or 335 nm (Figure 1; *25*−*27*). Surprisingly, the absorption spectrum of K69A ODC is identical to that observed for wild-type ODC (*22*), suggesting that the PLP aldehyde is not the species bound to the enzyme active site (Figure 2A). The possible explanations for this finding are the following: (1) In the absence of Lys-69, PLP forms a Schiff base with another Lys in the active site. (2) The purified enzyme is tightly bound to an exogenous amine. To distinguish between these possibilities the following studies were performed.

Reduction of wild-type and K69A ODC by sodium borohydride was performed to trap PLP covalently to the enzyme active site. After reduction, the enzymes were

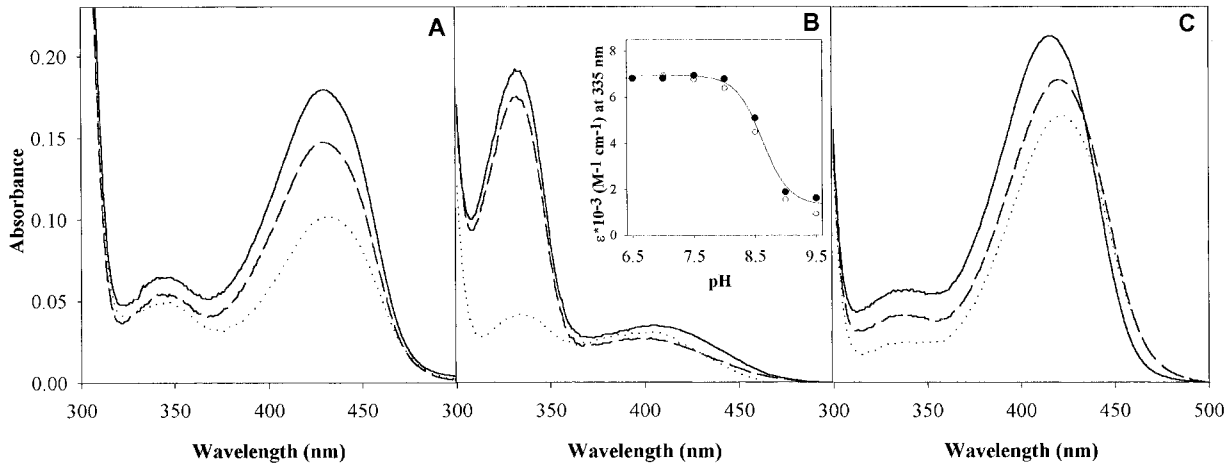

FIGURE 2: Spectral analysis of K69A and K69R ODC. (A) Spectra of PLP bound to K69A ODC (30 μM). (B) Spectra of PLP bound to K69R ODC (30 μM). The inset shows the pH dependence of milimolar absorptivities at 335 nm. Experimentally measured values (○) were corrected for PLP dissociation (●) and were fitted to eq 1 as described in Experimental Procedures. The parameters calculated from the fit (solid line) are pK_a = 8.62 ± 0.05, ϵ_{EH} = 6.95 ± 0.17 mM^{-1} cm^{-1}, and ϵ_E = 1.32 ± 0.19 mM^{-1} cm^{-1}. (C) Spectra of PLP bound to K69R ODC (30 μM) in the presence of 10 mM putrescine. Spectra were acquired at pH 6.5−9.5 in 0.1 M Hepes or Bicine and corrected for free PLP using ultrafiltration as described (*22*). Representative spectra at pH 7.0 (solid line), at pH 8.0 (dashed line), and at pH 9.0 (dotted line) are shown.

denatured in urea to release noncovalently associated cofactor. Free cofactor was removed by dialysis, and spectral analysis was performed on the denatured protein. For wild-type ODC, a spectral band was observed at 325 nm, consistent with the covalent attachment of PLP through an amine bond to a Lys residue (data not shown). In contrast, no spectral band was observed for K69A ODC in the region expected for enzyme-bound PLP. Therefore, we conclude that the unusual spectral properties of K69A ODC do not arise through formation of a Schiff base species with an alternate Lys in the active site.

To assess the possibility that exogenous amines are tightly bound to the active site of K69A ODC, reduction with sodium borohydride was performed on K69A and wild-type ODC, in the absence and presence of added putrescine (40 mM). The enzymes were denatured in urea, and the free PLP−amine adducts were separated from the protein by ultrafiltration. The PLP−amine adducts were then analyzed by anion-exchange column chromatography (Experimental Procedures). The retention times of the isolated adducts were compared to those of standards.

For wild-type ODC no PLP−amine adducts were isolated in the absence of added putrescine, consistent with the interpretation that 100% of the PLP was bound to Lys-69 during the reduction. In the presence of added putrescine, 100% of the PLP is isolated as the PLP−putrescine adduct (peak A, retention time 157 s). In contrast for K69A ODC, in the absence of added putrescine, three peaks are observed after anion-exchange chromatography. On the basis of retention times of the products, peak A (28% of the total) was identified as the PLP−putrescine adduct and peak C (38% of the total, retention time 337 s) as pyridoxine 5′-phosphate (the reduced aldehyde of PLP). Peak B (34% of the total, retention time 263 s) does not migrate with the same retention time as any of the controls but elutes with a retention time similar to those of PLP adducts with monoamines or diamino acids and most likely arises from the adduct of PLP with an uncharacterized amine. Addition of putrescine to K69A ODC converts peak C to the PLP−putrescine adduct; however, the exogenous amine (represented by peak B) is apparently too tightly bound to be displaced by added putrescine during the tested time course. Thus, for this preparation of K69A ODC, 34% of enzyme-bound PLP was present as the aldehyde species and 66% was bound to exogenous amines. These results explain the spectral profile of K69A ODC (Figure 2A). The finding that K69A ODC binds tightly to exogenous amines complicates detailed kinetic analysis of this mutant, and further analysis was carried out using the K69R ODC mutant (below).

Spectral Analysis of K69R ODC. In contrast to K69A ODC, the K69R ODC mutant displays spectral properties (Figure 2B; λ_{max} = 335 nm) that are consistent with the aldehyde species of PLP (Figure 1; *25*−*27*). The binding of putrescine to K69R ODC causes a decrease in absorbance at 335 nm and an increase at 415 nm, a change that is characteristic of the reaction of an amine with the PLP aldehyde, further supporting this assignment (Figure 2C). The final spectrum of the external aldimine is identical to that observed for wild-type ODC bound to putrescine (*22*).

At high pH the absorption band at 335 nm, of the uncomplexed enzyme, decreases in intensity (Figure 2B). The minimal model describing the pH titration behavior of K69R ODC requires the simultaneous dissociation of two protons (eq 1), both with pK_a = 8.5. These results suggest that the predominant PLP tautomer at neutral pH is the species that is protonated on both the pyridine nitrogen and on the 2′ hydroxyl (Figure 1; cationic ring, λ_{max} = 335 nm). At high pH the proton on the pyridine nitrogen dissociates giving rise to the neutral species (neutral ring, λ_{max} = 290 nm). Spectral analysis of wild-type *T. brucei* ODC also suggested that the proton on the pyridine nitrogen titrates with a pK_a of 8.5 (*22*).

The spectral properties of K69R ODC are unusual. An absorption maximum of 335 nm has been observed for the aldehyde species of PLP in solution but has not previously been reported for this species bound to an enzyme active site. Mutation of the active site Lys residue in other PLP-dependent enzymes (e.g. aspartate aminotransferase; *28*) gives rise to a spectrum with a maximum of 390 nm, which

Table 1: Kinetic Analysis of the Reaction of K69R and Wild-Type *T. brucei* ODC with L-Orn and Putrescine[a]

	K69R ODC	wild-type ODC
A. Kinetic Analysis of the Reaction of ODC with L-Orn		
k_{cat} (s^{-1})	0.0031 ± 0.0003	15[b]
K_m (mM)	0.18 ± 0.40	0.4[b]
k_{decarb} (s^{-1})	0.016 ± 0.0005	20 at 4 °C[c]
$K_{m.decarb}$ (mM)	0.31 ± 0.024	0.34 at 4 °C[c]
B. Kinetic Analysis of L-Orn Binding to ODC		
$K_{EL'.Orn}$ (mM)	15 ± 3.0	nd
$k_{+2.Orn}$ (s^{-1})	0.74 ± 0.090	$>10^3$ [d]
$k_{-2.Orn}$ (k_{off}) (s^{-1})	0.0061 ± 0.0004	nd
$k_{on.Orn}$ (M^{-1} s^{-1})	37 ± 1.0	$>10^5$ [d]
$K_{d.Orn}$ (mM)	0.17 ± 0.012	nd
C. Kinetic Analysis of Putrescine Binding to ODC		
$K_{EL'.Put}$ (mM)	0.77 ± 0.13	nd
$k_{+2.Put}$ (s^{-1})	0.23 ± 0.020	nd
$k_{-2.Put}$ (k_{off}) (s^{-1})	0.0035 ± 0.0014	1−3 at 4 °C[c]
$k_{on.Put}$ (M^{-1} s^{-1})	300 ± 57	$>10^5$ [d]
$K_{d.Put}$ (mM)	0.007 ± 0.0003	0.12 ± 0.008

[a] All data were collected at 37 °C in 0.1 M Hepes pH 7.5 unless specified. Kinetic constants are as described in Scheme 5. k_{cat} and K_m are the overall steady-state parameters, k_{decarb} is the first-order rate constant for the decarboxylation step (as determined in the single turnover experiment), $K_{m.decarb}$ is the Michaelis parameter obtained for steps only up to the decarboxylation step, $K_{d.Orn}$ and $K_{d.Put}$ are the equilibrium dissociation constant for the formation of the Schiff base species between ODC and L-Orn or putrescine, k_{on} is an apparent second-order rate constant for the formation of the Schiff base from free enzyme and ligand, and k_{off} is the first-order rate constant for the decay of the Schiff base to free enzyme and ligand. Errors are the standard error to the fit. [b] Data taken from ref *22*. [c] Data at 4 °C were taken from ref *18*. [d] Data at 37 °C were estimated by stopped-flow multiwavelength analysis as described ref *18*. [e] nd, not determined.

is reported to arise from the dipolar ion of the aldehyde species of PLP (*25*−*27*; Figure 1).

Steady-State and Pre-Steady-State Kinetic Analysis of CO_2 Production during the Reaction of K69R and K69A ODC with L-Orn. Steady-state data for the reaction of K69R ODC with L-Orn were collected for a range of substrate concentrations at 37 °C by measurement of released $^{14}CO_2$ from 1-^{14}C-L-Orn. The reaction was followed for up to 15 turnovers. The k_{cat} for the reaction ($k_{cat} = 0.0031$ s^{-1}) is 5000-fold lower than for wild-type ODC, while the K_m for L-Orn is not significantly altered by the mutation (Table 1).

To determine which steps in the reaction pathway have been affected by the mutation of Lys-69, pre-steady-state kinetic analysis of the reaction of K69R ODC was undertaken. Data were collected at saturating L-Orn concentration (2.4 mM), over a time range of 30−3500 s, which encompasses both the pre-steady-state and steady-state components of the reaction. The reaction proceeds through two phases, an initial release of CO_2 (a "burst"), followed by a slower step that dominates the steady-state rate (Figure 3). The observation of a burst phase for CO_2 release suggests the reaction of L-Orn with K69A ODC can be minimally modeled by Scheme 4, where the rate of the decarboxylation step is faster than the rate of product release. The magnitude of the burst (π) was calculated from analysis of the steady state phase of the data (Figure 3; $\pi = 6.4$ μM). These data demonstrate that minimally 64% of the enzyme ($E_T = 10$ μM based on absorbance at 280 nm) is active, ruling out the possibility that the observed decarboxylation arises from a minor component of the enzyme preparation. However, on the basis of Scheme 4, the magnitude of the burst will

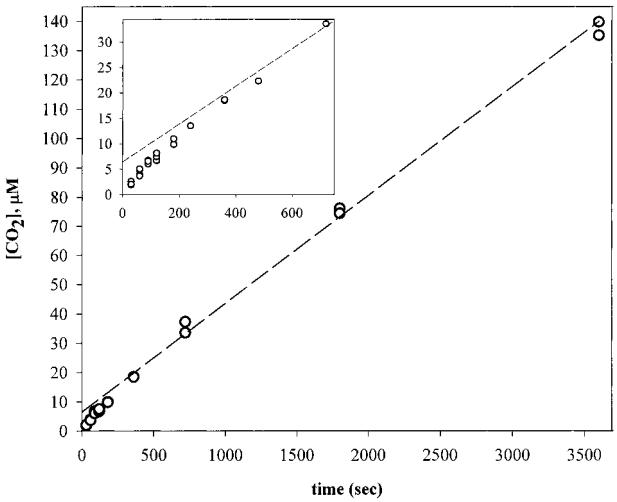

FIGURE 3: Pre-steady-state kinetic analysis of L-Orn decarboxylation by K69R ODC. K69R ODC (10 μM) was incubated with 1-[^{14}C]-L-Orn (2.4 mM) in 0.1 M Hepes buffer pH 7.5, 0.1 mM PLP, 1 mM DTT at 37 °C. Product formation (open circles) was determined by the [^{14}C]-CO_2 trapping assay. The steady-state phase of the reaction (720−3500 s) was approximated by linear regression (dashed line): $[CO_2] = \pi + [ODC]k_{cat}t$. The values of parameters determined by this analysis are π(or "burst") $= 6.4 \pm 1.2$ πM and $k_{cat} = 0.0037 \pm 0.0001$ s^{-1}. The inset shows the expanded region of the graph corresponding to the pre-steady-state phase of the reaction.

underestimate the active enzyme concentration, if k_{decarb} is not sufficiently larger than $k_{off.Put}$ (*29*). Single turnover kinetic analysis and spectral analysis of the reaction (below) demonstrate that the rate of decarboxylation is only 4-fold faster than the rate of product release. Thus, the measured value of the burst is consistent with the conclusion that 100% of K69R ODC is active and that the burst is suppressed by the similarity of the rate constants (k_{decarb} and $k_{off.Put}$).

Single Turnover Kinetic Analysis of the Reaction of K69R ODC with L-Orn. The quantitation of CO_2 formed under single turnover conditions allows the reaction steps up to and including decarboxylation to be isolated from the remaining reaction steps (e.g. product release). K69R ODC was incubated with 1-$^{14}CO_2$-Orn, under conditions where enzyme was present in large excess over substrate, and the rate of CO_2 production was measured (Experimental Procedures). The decay of 1-$^{14}CO_2$ from the reaction solution follows first-order kinetics, and the data were fitted to eq 2A to obtain k_{obs} (Figure 4). The k_{obs} values obtained at different enzyme concentrations were well fit by eq 2B (Figure 4 inset), which describes a one-step binding reaction followed by an irreversible decarboxylation step (Scheme 1). The kinetic parameters ($k_{decarb} = 0.016 \pm 0.0005$ s^{-1} and $K_{m.decarb} = 0.31 \pm 0.024$ mM; Table 1) were determined from the fit.

The first-order rate constant, k_{decarb}, represents the rate-limiting step up to and including the decarboxylation step. Assuming rapid formation of a Michaelis complex, this term could be limited by Schiff base formation or by decarboxylation. Minimally, the data suggest that the decarboxylation step occurred with a rate constant of 0.016 s^{-1} or greater. Analysis of the L-Orn binding kinetics (below) suggests that Schiff base formation is relatively fast, and therefore, the single turnover experiment allows for a direct measure of the rate of the decarboxylation step. The rate of the

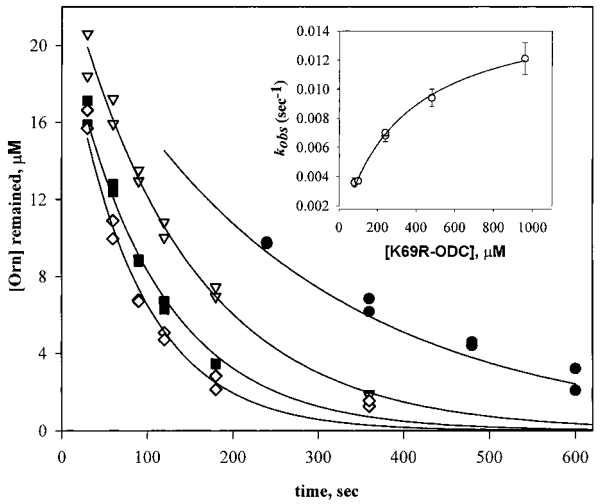

FIGURE 4: Single-turnover analysis of L-Orn decarboxylation by K69R ODC. 1-[^{14}C]-L-Orn (20 μM) was incubated with a 5−20 molar excess of K69R ODC in 0.1 M Hepes pH 7.5, at 37 °C. The remaining [^{14}C]-Orn was quantitated after quenching the reaction with acid as described in Experimental Procedures. Data were collected for various concentrations of K69R ODC, 0.1 mM (black circles), 0.24 mM (white inverted triangles), 0.5 mM (black squares), and 1.0 mM (white diamonds), and were fitted to eq 2A to obtain k_{obs} (solid lines). The inset shows the K69R ODC concentration dependence of k_{obs} (open circles) on enzyme concentration. $K_{m.decarb}$ = 0.31 ± 0.024 mM and k_{decarb} = 0.016 ± 0.0005 s^{-1} were determined from the fit of k_{obs} to eq 2B. The fit is shown by the solid line.

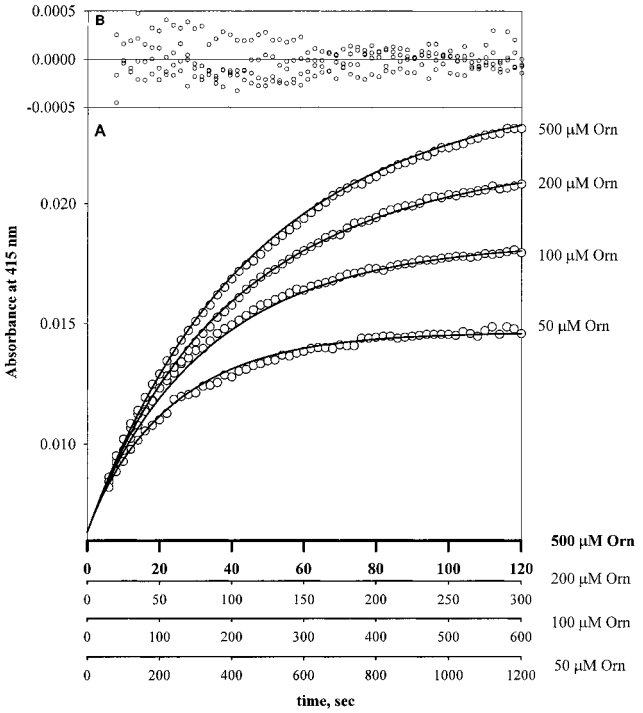

FIGURE 5: Spectral analysis of the reaction of L-Orn with K69R ODC. (A) Absorbance at 415 nm was monitored upon incubation of K69R ODC (3 μM) with L-Orn (0.05−0.50 mM) in 0.1 M Hepes buffer pH 7.5 and 1 mM DTT at 37 °C. The time intervals for data collection were varied with the concentration of L-Orn so that data could be acquired in both the pre-steady-state phase and the early steady-state phase at all concentrations. The data for each L-Orn concentration are displayed using an individual time scale, shown below the graph. The data for all four Orn concentrations were simultaneously fitted to eq 4. The simultaneous fit to all data points (open circles) is displayed by the solid lines. k_{decarb} was fixed at 0.016 s^{-1} during the fit, and the values of the remaining parameters were calculated from the fit to be $k_{off.Orn}$ = 0.0061 ± 0.0004 s^{-1}, $k_{on.Orn}$ = 37 ± 1 M^{-1} s^{-1}, $k_{off.Put}$ = 0.0026 ± 0.00003 s^{-1}, $\epsilon_{415\ nm}$ = 7.4 ± 0.06 mM^{-1} cm^{-1}, and A_0 = 0.0063 ± 0.00007. (B) The residuals from the fit to eq 4 are displayed at the different individual time scales, shown below the graph.

decarboxylation step (0.016 s^{-1}) is 5-fold faster than k_{cat} (0.0031 s^{-1}); thus, the decarboxylation step is not the rate-determining step in the reaction of K69R ODC with L-Orn. The rate of the decarboxylation step for wild-type ODC was previously measured to be 20 s^{-1} at 4 °C, by stopped-flow mulitiwavelength spectroscopy (*18*). This rate constant was estimated to be 10-fold faster at 37 °C by the same methods. Thus, in comparison to the wild-type enzyme, the rate of the decarboxylation step catalyzed by K69R ODC has decreased on the order of 10^4-fold.

Spectral Analysis of the Reaction of L-Orn with K69R ODC. The reaction of K69R ODC with L-Orn was initially followed on a diode array spectrophotometer over the absorbance range of 300−500 nm. Similarly to putrescine, the binding of L-Orn to K69R ODC causes a decrease in the absorbance at 335 nm and an increase at 415 nm. For wild-type ODC, in addition to changes in these absorption bands, an additional band appears at 450 nm during the course of the reaction with L-Orn; this spectral band was assigned to the quinoid intermediate that occurs upon decarboxylation (*18*). No additional spectral band is observed for K69R ODC; thus, subsequent analysis of the reaction time course (12−1200 s) with L-Orn was performed at a single wavelength (415 nm).

At low L-Orn concentration (0.050−0.5 mM), the observed rate constant (k_{obs}) for the change in absorbance at 415 nm has a linear dependence on L-Orn concentration, and Schiff base formation was modeled by a single-step process. Schiff base formation is followed by the decarboxylation and product release steps, thus, the minimal model that describes the reaction with L-Orn under these conditions is depicted in Scheme 4. Assuming that the extinction coefficients of E-Orn and E-Put, at 415 nm, are identical ($\epsilon_{E-Orn} \approx \epsilon_{E-Put}$), eq 4 describes the sum of both spectrally detectable enzyme forms (E.Orn + E.Put), and was used to model the time dependence of the absorbance change during the reaction with L-Orn. This assumption is supported by the observation that the extinction coefficients at 415 nm for K69R ODC bound to putrescine and D-Orn are the same (data not shown). The data collected at four separate L-Orn concentrations were globally fitted to eq 4. Three kinetic parameters ($k_{on.Orn}$, $k_{off.Orn}$, and $k_{off.Put}$) and two amplitude factors (the average ([E-Orn] + [E-Put]) extinction coefficient (ϵ) and the initial absorbance at 415 nm), were determined from the fit (Table 1 and Figure 5). k_{decarb} was fixed during the fit at the value determined by single-turnover assay (0.016 s^{-1}) described above. The overall dissociation constant ($K_{d.Orn}$ = 0.17 ± 0.012 mM) for the Schiff base species between L-Orn and K69R ODC was determined from the ratio of $k_{off.Orn}/k_{on.Orn}$. To assess the quality of the model, additional fits to the data were undertaken in which the ratio of $k_{off.Orn}$ /$k_{off.Put}$ was fixed at levels above and below the ratio predicted in the global fit. The only ratio of these parameters that gave a good fit to the data was the value determined from the global fit, $k_{off.orn}$ /$k_{off.Put}$ close to 1. Further, $k_{off.Put}$ (0.0026 s^{-1}) predicted by this model is in good agreement with the value determined

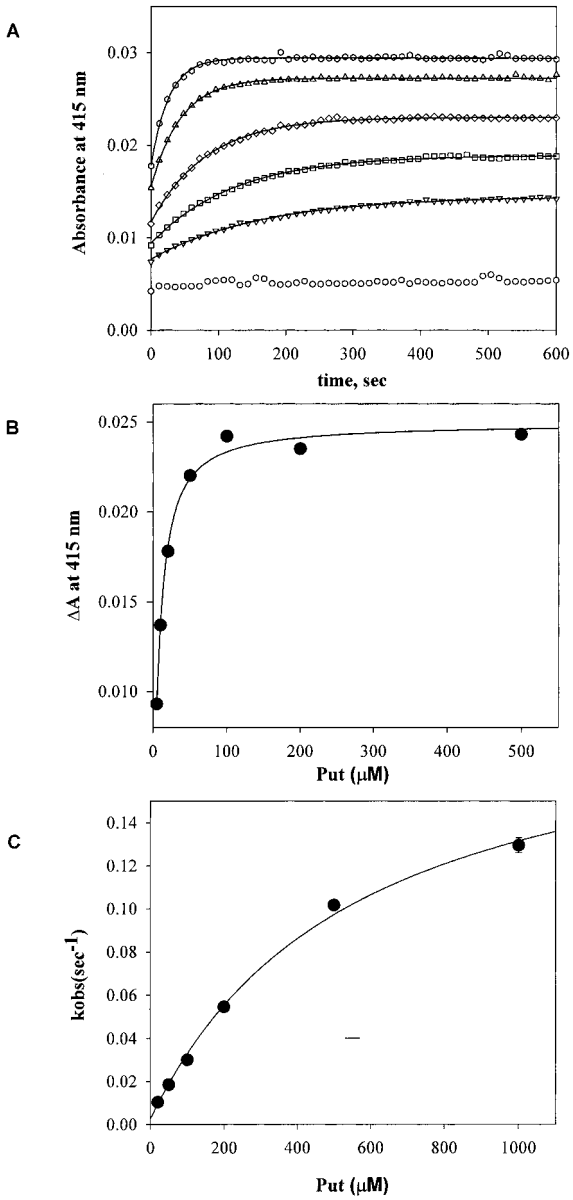

FIGURE 6: Spectral analysis of the binding of putrescine to K69R ODC. (A) Absorbance at 415 nm (symbols) was monitored upon incubation of K69R ODC (3 μM) with putrescine (0.005−1.0 mM) in 0.1 M Hepes buffer pH 7.5, at 37 °C. The data were fitted to eq 3A, to obtain the values of k_{obs} and ΔA_{415nm}. The curves predicted by the fit are shown by the solid lines. Data points are represented as follows: no putrescine (○) without a line; 0.005 mM putrescine (▽); 0.01 mM putrescine (□); 0.02 mM putrescine (◇); 0.05 mM putrescine (△); 0.1 mM putrescine (○). The zero time point is equal to the dead time of mixing (~3 s). (B) The putrescine concentration dependence of the amplitude parameter, ΔA_{415nm} (symbols). The data (solid circles) were fitted to eq 3C (solid line) to determine the dissociation binding constant. The values of the parameters determined by the fit (solid line) are $K_d = 0.007 \pm 0.0003$ mM and $\epsilon_{415nm} = 8.3 \pm 0.1$ mM^{-1} cm^{-1}. (C) The putrescine concentration dependence of the observed pseudo-first-order rate constant (k_{obs}). The data (solid circles) were fitted to eq 3D (solid line) to determine the kinetic parameters for the binding reaction ($k_{+2.Put} = 0.23 \pm 0.02$ s^{-1}, $k_{-2.Put} = 0.0035 \pm 0.0014$ s^{-1}, $K_{ES'} = 0.77 \pm 13$ mM.

by spectral analysis of putrescine binding (Table 1 and Figure 6).

At high concentrations of L-Orn (2−25 mM), a hyperbolic dependence of k_{obs} on L-Orn concentration was observed. Under these conditions, a two-step model is required to describe Schiff base formation, providing kinetic evidence that an intermediate (E-Orn′) is formed prior to the Schiff base species (E-Orn). Since the rate of Schiff base formation is fast compared to k_{decarb} and $k_{-2.Orn}$, it was assumed that these latter steps do not significantly contribute to the absorbance changes within the measured time course, and the data were fitted to a two-step binding model with a rapid equilibrium first step (Scheme 2, eq 3D). A considerably higher concentration of substrate is required to saturate the kinetic intermediate ($K_{EL'} = 15$ mM) than the Schiff base species ($K_{d.Orn} = 0.17$ mM). The intermediate decays to the Schiff base species with a rate constant ($k_{+2.Orn} = 0.74$ s^{-1}) that is 50-fold faster at saturation than the rate constant measured in the single turnover experiment. The ratio of $k_{+2.Orn}/K_{EL'.Orn}$ provides another measure of $k_{on.Orn}$, and the value calculated by this ratio (49 M^{-1} s^{-1}) is in reasonable agreement with the value (37 M^{-1} s^{-1}; Table 1) calculated using the full model (Scheme 4, eq 4) at low L-Orn concentrations.

Finally, the kinetics of L-Orn binding to wild-type ODC are too rapid to be accurately measured at 37 °C. However, estimates of $k_{on.Orn}$ were made by stopped-flow multiwavelength kinetic analysis of the wild-type reaction, using the same methods as were previously reported for analysis at 4 °C (*18*). On the basis of this analysis, $k_{on.Orn}$ has decreased by at least 10^3-fold for K69R ODC in comparison to the wild-type enzyme (Table 1).

Spectral Analysis of Putrescine Binding to K69R ODC. The reaction of K69R ODC with putrescine was followed (0−600 s) at 415 nm for a range of putrescine concentrations (0.005−1 mM), and the data were fitted to eq 3A to obtain both the amplitude at equilibrium and rate (k_{obs}) factors (Figure 6A). The equilibrium dissociation constant ($K_{d.Put}$) for the formation of the Schiff base species between enzyme-bound PLP and putrescine was determined from analysis of the amplitude data, using eq 3C (Figure 6B and Table 1), to be 0.007 mM. The k_{obs} data were fitted to eq 3D which describes a two-step binding model (Scheme 2), with a rapid equilibrium first step, to obtain the kinetic parameters ($K_{EL'}$, $k_{+2.Put}$, and $k_{-2.Put}$) of putrescine binding (Figure 6C and Table 1). The values of $k_{on.Put}$ and $k_{off.Put}$ were determined from these parameters. The first-order rate constant for putrescine dissociation ($k_{-2.Put} = 0.0035$ s^{-1}) is very similar to the overall k_{cat} (0.0031 s^{-1}); thus, as for the wild-type enzyme (*18*), product release is the predominant rate-limiting step for catalysis by K69R ODC.

Analysis of the reaction of wild-type ODC with putrescine at 37 °C by stopped-flow multiwavelength spectroscopy sets the lower limit for $k_{on.Put}$ to be 10^5 M^{-1} s^{-1} and $k_{off.put}$ was estimated to be 10-fold faster than the rate observed at 4 °C. Thus, in comparison to the wild-type enzyme, $k_{off.Put}$ is decreased approximately10^4-fold by mutation of Lys-69 to Arg and $k_{on.Put}$ is decreased minimally by 10^3-fold. These data demonstrate that Lys-69 plays a significant role in accelerating both the rates of Schiff base formation and decay.

CD Analysis of the Binding of Putrescine to Wild-Type ODC. For wild-type ODC the absorbance changes observed at 335 and 420 nm upon binding of substrate or product are small in comparison to those for K69R ODC. However, changes in the CD signal that arise from enzyme-bound PLP are observed upon binding of putrescine to either wild-type

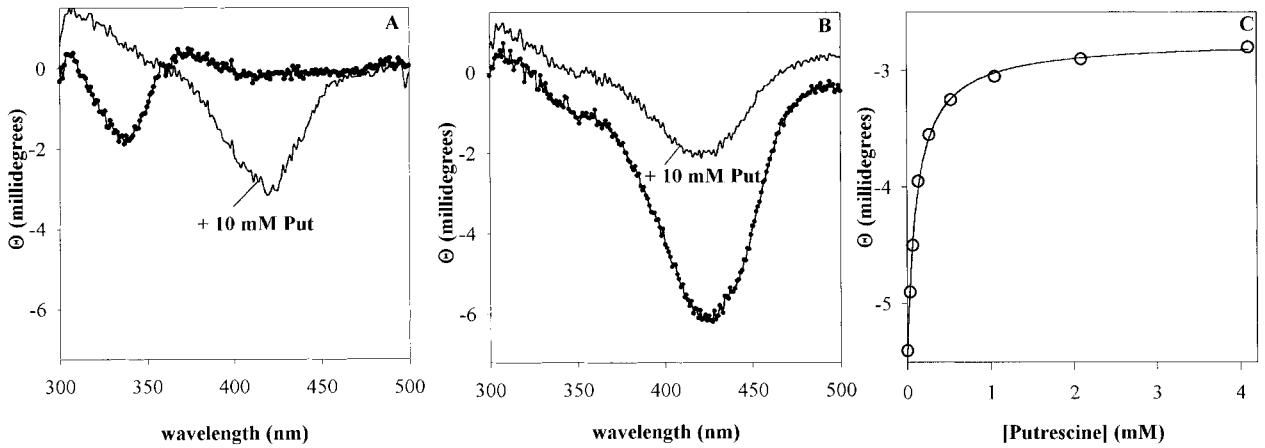

FIGURE 7: CD spectral analysis of putrescine binding to K69R and wild-type ODC at 420 nm. (A) K69R ODC (30 μM) before (●) and after (−) incubation with 10 mM putrescine in 0.1 M Hepes buffer pH 7.5. (B) Wild-type ODC (30 μM) before (●) and after (−) incubation with 10 mM putrescine under the same conditions. (C) Titration of the CD spectra at 420 nm (circles) upon incubation of wild-type ODC with putrescine. The data (○) were fitted to eq 5 (line) to calculate the dissociation binding constant for putrescine ($K_{d,Put}$ = 0.12 ± 0.008 mM).

Table 2: Dissociation Constants for the Binding of Diamines to ODC and Free PLP[a]

		K_d (mM)		
ligand	pK_a	wild-type ODC	K69R ODC	free PLP
1,2-diaminoethane	7.1	16.1 ± 1.8 (130)	1.6 ± 0.1 (230)	0.078 ± 0.003 (0.4)
1,3-diaminopropane	8.5	16.2 ± 0.8 (130)	0.27 ± 0.009 (40)	0.14 ± 0.004 (0.7)
putrescine	9.2	0.12 ± 0.008 (1)	0.007 ± 0.0003 (1)	0.20 ± 0.017 (1)
cadaverine	10.0	4.7 ± 1.6 (40)	0.15 ± 0.006 (20)	0.36 ± 0.028 (2)
1,6-diaminohexane	9.8	24 ± 3.6 (200)	0.076 ± 0.01 (10)	0.74 ± 0.08 (4)
1,7-diaminoheptane	*b*	42 ± 3.2 (350)	1.1 ± 0.06 (150)	0.61 ± 0.047 (3)

[a] K_d represents the dissociation binding constant for the formation of the Schiff base species and is based on the molar concentration of diamine. Values in parentheses are relative affinities normalized to Put ($K_{d,L}/K_{d,Put}$). Errors are the standard error to the fit. The K_d's for K69R ODC and free PLP were determined by absorbance spectroscopy at 415 nm. The K_d's for wild-type ODC were determined by CD spectroscopy at 420 nm. All data were collected in 0.1 M Hepes pH 7.5 at 37 °C. pK_a data were taken from ref *37*. [b] Data were not available.

or K69R ODC (Figure 7). The dissociation constant ($K_{d,Put}$) for wild-type ODC was obtained by measurement of the change in elipticity at 420 nm upon putrescine binding, and by fitting of the data to eq 5. Putrescine binds 17-fold tighter to K69R ODC than wild-type ODC.

Ligand Specificity of Wild-Type and K69R ODC. Wild-type ODC has a strong preference for L-Orn over other basic amino acids; the k_{cat}/K_m for L-Orn was found to be 100-fold higher than for L-Lys and 1000-fold higher than for L-Arg, while decarboxylation of diaminobutyric acid could not be detected (*30*). After these studies, HPLC analysis of our commercial L-Arg stocks demonstrated that they were contaminated with up to 1% L-Orn. On the basis of direct detection of agmatine by HPLC assay, we have redetermined the kinetic parameters of the reaction with L-Arg (K_m = 14 ± 3 mM and k_{cat} = 0.025 ± 0.002 s^{-1}). These data confirm that *T. brucei* ODC catalyzes the decarboxylation of L-Arg at a greatly reduced efficiency compared to L-Orn. However, our previously reported kinetic data, based on measurement of CO_2 (*30*), overestimated the k_{cat}/K_m of the reaction by 16-fold. Decarboxylation of amino acids other than L-Orn could not be detected for K69R ODC.

Binding analysis of a series of diamines and amino acids was undertaken and compared to the reaction with free PLP. Data were collected and analyzed by absorbance (K69R ODC or free PLP) or CD (wild-type) spectroscopy as described for putrescine. Wild-type and K69R ODC have similar specificity and preferentially bind Put 10−400-fold more tightly than the shorter or longer diamines, though K69R ODC binds all diamines 10−100-fold more tightly than the wild-type enzyme (Table 2). D-Orn and putrescine bind with similar affinity to both K69R and wild-type (K_d = 0.27 ± 0.01 mM) ODC, and both bind with higher affinity to K69R ODC than L-Orn (Tables 1 and 2).

For the binding of the diamines to K69R ODC, the dependence of k_{obs} on ligand concentration was hyperbolic, while for free PLP saturation of k_{obs} vs diamine concentration was only observed for diaminopropane and putrescine. For K69R ODC, the equilibrium dissociation constant for the EL′ intermediate (K_{EL}') is 6−50-fold lower for putrescine, than for the other diamines, paralleling the results observed for the overall K_d for Schiff base formation (Tables2 and 3). The rate of conversion from the EL′ intermediate to the Schiff base species (k_{+2}) is very similar for the series of diamines tested and does not represent a step in which further binding specificity is achieved. Further, the k_{+2} values measured for the reaction of free PLP with diaminopropane and putrescine are very similar to the values determined for their reaction with K69R ODC.

The higher affinity binding of K69R ODC allowed analysis of a wider range of functional groups than for the wild-type enzyme, and the binding analysis of K69R ODC was extended to a series of amino acids. K69R ODC binds Orn and analogues (L-Orn, D-Orn, and AMO) 10^3−10^4-fold more tightly then the weakest binding amino acid (L-Ala), while for free PLP only a 250-fold difference is observed between the best and worst binding amino acids (Table 4). The K_d's for Schiff base formation between the L-amino acids and

Table 3: Kinetic Analysis of the Binding of Diamines to K69R ODC and to Free PLP[a]

	K69R ODC				free PLP			
ligand	$K_{EL'}$ (mM)	k_{+2} (s^{-1})	k_{on} (M^{-1} s^{-1})	k_{off} (s^{-1})	$K_{EL'}$ (mM)	k_{+2} (s^{-1})	k_{on} (M^{-1} s^{-1})	k_{off} (s^{-1})
1,3-diaminopropane	4.3 ± 0.40	0.31 ± 0.013	72 ± 7.4	0.023 ± 0.0013	4.5 ± 0.90	0.6 ± 0.07	130 ± 31	0.018 ± 0.004
putrescine	0.77 ± 0.13	0.23 ± 0.02	300 ± 57	0.0035 ± 0.0014	8.3 ± 2.0	0.37 ± 0.04	45 ± 12	0.0072 ± 0.0033
cadaverine	12 ± 2.0	0.35 ± 0.030	29 ± 5.5	0.007 ± 0.0009	na	na	15 ± 0.4	0.0060 ± 0.0002
1,6-diaminohexane	5.7 ± 0.40	0.35 ± 0.014	61 ± 5.0	0.003 ± 0.0009	na	na	6.3 ± 0.4	0.0094 ± 0.001
1,7-diaminoheptane	38 ± 6.0	0.12 ± 0.011	3.0 ± 0.60	0.0060 ± 0.0004	na	na	6.9 ± 0.2	0.0060 ± 0.0003

[a] Binding kinetics were monitored by absorbance measurements at 415 nm in 0.1 mM Hepes pH 7.5 at 37 °C. Kinetic constants were calculated as described in Experimental Procedures. Kinetic parameters are defined in Schemes 2 and 3. na = not applicable as a linear dependence of k_{obs} on ligand concentration was observed. The binding kinetics of diaminoethane were too fast for analysis. Errors are the standard error of the fit.

Table 4: Kinetic and Equilibrium Analysis of the Binding of Amino Acids to K69R ODC and Free PLP[a]

		K_d (mM)		k_{on} (M^{-1} s^{-1})		k_{off} (s^{-1})	
ligand	pK_a	K69R-ODC	PLP	K69R-ODC	PLP	K69R-ODC	PLP
Dapa	6.7	1.7 ± 0.30	0.13 ± 0.021	33 ± 12	nd	0.086 ± 0.007	nd
Daba	8.2	0.71 ± 0.072	0.38 ± 0.020	10 ± 0.89	39 ± 2.8	0.0066 ± 0.0006	0.026 ± 0.0060
L-Orn	8.7	0.16 ± 0.012	0.68 ± 0.060	37 ± 1.0	18 ± 1.2	0.0061 ± 0.0004	0.016 ± 0.0055
D-Orn	8.7	0.011 ± 0.0007	0.60 ± 0.080	53 ± 3.3	20 ± 0.4	0.0004 ± 0.0002	0.015 ± 0.0009
Amo	*	0.27 ± 0.017	1.0 ± 0.065	4.1 ± 0.10	7.8 ± 0.10	0.0007 ± 0.0001	0.010 ± 0.0004
L-Lys	9.2	0.78 ± 0.055	1.5 ± 0.17	1.8 ± 0.030	3.9 ± 0.10	0.0023 ± 0.0002	0.0084 ± 0.0005
Dpma	8.8	2.9 ± 0.32	1.7 ± 0.10	0.23 ± 0.004	5.0 ± 0.10	0.0011 ± 0.00003	0.011 ± 0.0007
L-Arg	9.0	1.6 ± 0.18	1.3 ± 0.055	1.4 ± 0.010	70 ± 0.20	0.0035 ± 0.0002	0.010 ± 0.0006
L-His	9.3	0.99 ± 0.073	4.0 ± 0.80	2.1 ± 0.28	7.1 ± 0.30	0.0022 ± 0.0001	0.024 ± 0.0018
L-Ala	9.9	63 ± 11	33 ± 3.0	0.065 ± 0.004	0.60 ± 0.040	0.0045 ± 0.0002	0.018 ± 0.0014
Aba	9.8	29 ± 7.0	12 ± 1.0	0.090 ± 0.017	0.90 ± 0.040	0.0028 ± 0.0003	0.011 ± 0.0009
L-Met	9.3	2.6 ± 0.20	8.3 ± 1.0	0.24 ± 0.006	2.1 ± 0.10	0.0008 ± 0.0001	0.017 ± 0.0009
L-Phe	9.3	1.9 ± 0.15	5.0 ± 0.35	0.36 ± 0.010	2.7 ± 0.20	0.0005 ± 0.00004	0.017 ± 0.002

[a] Dapa, L-2,3-diaminopropionic acid; Daba, D,L-2,4-diaminobutyric acid; Dpma, L-α,ϵ-diaminopimelic acid; Aba, L-α-aminobutyric acid; Amo, α-methylornithine. K_d is the dissociation binding constant for the Schiff base species, k_{on} is the apparent second-order rate constant for formation of the Schiff base, and k_{off} is the first-order rate constant for the decay of the Schiff base to free ligand (Scheme 3). Two-step binding kinetics (Scheme 2) were observed for the binding of L-Orn (see Table 2), D-Orn, Dapa, and Daba to K69R ODC. The data were fitted to eq 3D to determine the values of $K_{EL'}$ (D-Orn (5.7 mM), Dapa (13 mM), and Daba (41 mM)) and k_{+2} (D-Orn (0.3 s^{-1}), Dapa (0.43 s^{-1}), and Daba (0.42 s^{-1})). Binding kinetics were monitored by absorbance at 415 nm in 0.1 M Hepes pH 7.5 at 37 °C. Kinetic constants were obtained as described in Experimental Procedures. pK_a data were taken from ref *37*. * No data available. Errors are the standard error of the fit.

K69R ODC are 10−25-fold higher than for the corresponding diamines (L-Orn/putrescine; L-Lys/cadaverine; Daba/diaminopropane). Further K69R ODC binds D-Orn with 15-fold higher affinity than L-Orn, yet D-Orn was not decarboxylated. These findings suggest that ODC promotes decarboxylation of L-Orn by destabilizing interactions with the α-carboxylate.

A linear dependence of k_{obs} on amino acid concentration was observed for the binding of all amino acids to free PLP and to K69R ODC (Scheme 3), with the exception that for K69R ODC saturation was observed for L-Orn, D-Orn, Dapa, and Daba (Table 4 footnote). Comparison of the rates of Schiff base decay (k_{off}) for the series of diamines and amino acids demonstrates that little variation in k_{off} occurs within each series for either K69R ODC or free PLP (Tables 3 and 4). Diamine and amino acid specificity by the enzyme is primarily manifest during Schiff base formation; k_{on} was accelerated by the enzyme relative to PLP for only the physiological ligands, (e.g. L- and D-Orn and putrescine), while for the nonphysiological ligands k_{on} was generally faster for binding to free PLP than to K69R ODC.

DISCUSSION

A common feature among all PLP-dependent enzymes is the presence of an active site Lys residue that forms a Schiff base with the cofactor in the absence of substrate. A Lys residue is invariant despite the fact that the PLP-dependent enzymes can be classified into four independent structural classes (*6*). In this paper the role of this residue (Lys-69) in catalysis by the eukaryotic ODC's has been defined by detailed kinetic analysis of the K69R mutant of *T. brucei* ODC. The K69R ODC mutant was chosen as a better model than the K69A mutant for detailed kinetic analysis, based on the finding that a substantial fraction of purified K69A ODC bound tightly to exogenous amines. These results complicate spectral analysis of the reaction steps, making K69A ODC a poor model for detailed kinetic studies. The K87T mutant of tryptophan synthase also binds amino acids with high affinity such that complexes could be isolated by gel filtration (*13*). In contrast, spectral analysis suggests that PLP is bound to K69R ODC as the free aldehyde. The rate of the single turnover reaction catalyzed by K69A ODC (data not shown) was similar to that measured for K69R ODC (Figure 4). These data provide evidence that mutation of K69 to the bulkier Arg residue is well tolerated in the active site and that K69R ODC is a suitable model for analysis of the role of Lys-69 in catalysis.

Characterization of the reaction of both substrate (L-Orn) and product (putrescine) with K69R ODC allows an overall model to be proposed for the reaction pathway (Scheme 5). Spectral analysis of the binding of L-Orn and putrescine is consistent with a two-step binding mechanism to form the Schiff base species (E-Orn or E-Put) with K69R bound PLP. The data are well modeled by assuming a rapid equilibrium with the first intermediate (E-Orn′), followed by slower

Scheme 5: Mechanisms of Decarboxylation by ODC

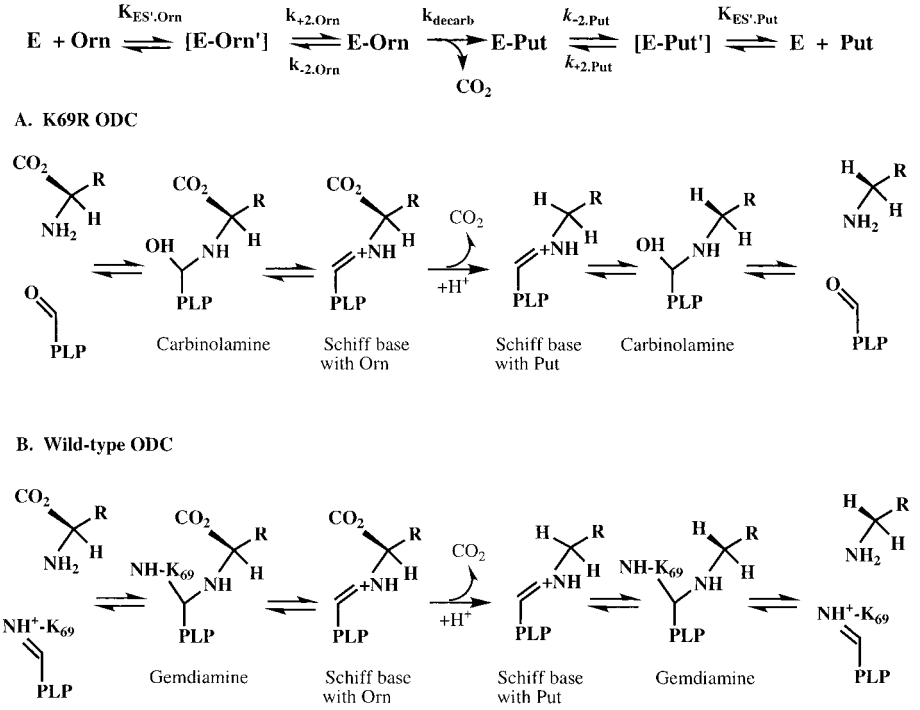

formation (e.g. $k_{+2.Orn} = 0.74\ s^{-1}$) of the Schiff base species. Once the Schiff base with L-Orn forms, decarboxylation occurs at a rate ($k_{decarb} = 0.016\ s^{-1}$) that is 50-fold slower than the previous step at saturation (Table 1). As for wild-type ODC (*18*), the overall rate-limiting step in the reaction is product release ($k_{off.put} = 0.0035\ s^{-1}$). Multiwavelength UV/vis spectral analysis of the reaction of wild-type ODC with L-Orn provided evidence that a quinoid intermediate forms upon decarboxylation and decays with a rate constant that is at least 10-fold greater than the decarboxylation step (*18*). In contrast, for K69R ODC no spectral evidence for the quinoid intermediate is found, suggesting that the rate of quinoid decay, which minimally must include protonation of C_α, is faster relative to the rate of its formation than for the wild-type enzyme. In contrast, for aspartate aminotransferase, the quinoid intermediate is not observed in the wild-type reaction but is observed for the reaction of substrate with the K258R mutant enzyme (*28*).

For wild-type ODC Schiff base formation proceeds through a gem diamine intermediate (Scheme 5), whereas Schiff base formation between amines and the free PLP aldehyde occurs via the formation of a carbinolamine intermediate (*31*). This latter mechanism would be expected to operate for K69R ODC as well. In addition, for the reactions of ligands with enzyme-bound PLP, the formation of a noncovalent enzyme/ligand intermediate (e.g. the Michaelis complex for substrate) must precede the chemical steps. Therefore, for K69R ODC bound PLP, the kinetic intermediate (EL′) observed prior to Schiff base formation could be either the carbinolamine intermediate or the Michaelis complex. Analysis of the kinetics of binding of the diamines, putrescine, and diaminopropane, to both free PLP and K69R ODC, suggests that the initial observed intermediate is in fact the carbinolamine. For these diamines, the rate constant (k_{+2}) for the conversion of the EL′ intermediate to the Schiff base species is strikingly similar between K69R ODC and free PLP (Table 3), providing evidence that ES′ represents a common intermediate. Since the Michaelis complex is not shared in common between the reaction of diamines with free PLP and the reaction with K69R ODC, these data support the conclusion that the kinetic intermediate is the carbinolamine intermediate.

In comparison to the wild-type enzyme, the rates of formation and decay of the Schiff base species have been significantly decreased by mutation of Lys-69 to Arg, demonstrating that a major role of Lys-69 is to accelerate these steps. We estimate that mutation of Lys-69 in ODC decreases $k_{on.Put}$ and $k_{on.Orn}$ by at least 10^3-fold, such that the rates of Schiff base formation between putrescine or L-Orn and K69R ODC have been slowed to within 1 order of magnitude of the uncatalyzed rate with free PLP (Tables 1−3). Similar effects on Schiff base formation have been reported for both aspartate aminotransferase (*10*) and tryptophan synthase (*13*) upon mutation of the catalytic Lys in these enzymes. The apparent second-order rate constants (k_{on}) for the formation of the Schiff base between K69R ODC and L-Orn or putrescine ($40-300\ M^{-1}\ s^{-1}$) are similar to the values measured for the rate of Schiff base formation between K258A aspartate aminotransferase and Glu or Asp ($300-2000\ M^{-1}\ s^{-1}$).

For ODC the off rate of putrescine ($k_{off.put}$) is decreased by 10^4-fold upon mutation of Lys-69 to Arg, to a value that is identical to the rate observed for dissociation of putrescine from free PLP (Table 3). The observation that putrescine, D-Orn, and the other tested diamines bind with higher affinity to K69R ODC than to the wild-type enzyme is consistent with the conclusion that the mutation has a larger effect on Schiff base hydrolysis than Schiff base formation.

For many PLP-dependent enzymes, the Lys residue plays an essential role as the catalytic base to abstract the α-proton in the first chemical step of the reaction. For example, mutation of K258A in aspartate aminotransferase decreased the rate of this step by 10^6-10^8-fold (*8*). Instead, for the PLP-dependent decarboxylases, the enzyme catalyzes bond

cleavage between C_α and the α-carboxylate, suggesting that the Lys residue would not be essential for this step. Yet, for ODC the rate of the decarboxylation step decreased by $\sim 10^4$-fold upon mutation of Lys-69 to Arg. Greater stability of the external aldimine species in K258A aspartate aminotransferase was proposed to account for differences in enzyme reactivity in comparison to the wild-type enzyme (*10*). Our data on ODC indicate that the external aldimine formed between putrescine and K69R ODC is 1.7 kcal/mol more stable than for the wild-type enzyme. Further, we find that a series of diamines and D-Orn also bind more tightly to K69R ODC than to the wild-type enzyme. If this trend holds for L-Orn (the magnitude of $K_{d.Orn}$ could not be determined for the wild-type enzyme), attainment of the transition state for decarboxylation might be made more difficult because of the greater stability of the prior enzyme-bound intermediate. However, this effect is not large enough to fully explain the decreased rate of decarboxylation. Lys-69 may play a role in the orientation of the α-carboxylate relative to the imine bond. The precise orientation of the scissile bond has been proposed to control reactivity in PLP-dependent enzymes (*32*).

While Lys-69 plays an essential catalytic role in accelerating Schiff base formation and hydrolysis, it does not mediate substrate specificity. The binding data collected for the series of diamines and D-Orn demonstrate that wild-type and K69R ODC have similar ligand specificity, even though K69R ODC binds ligands more tightly than the wild-type enzyme. Free PLP binds amino acids and diamines with a range of affinities; however, almost all of the selectivity can be attributed to differences in the pK_a of the ligand amino group. When the K_d's are recalculated to reflect the concentration of free base ($K_{d.fb} = K_d/(1 + 10^{(pK_a - pH)})$), free PLP binds the free base of all the tested ligands with very similar affinity (within a factor of 4). A component of the ligand specificity of K69R ODC is also clearly associated with this pK_a effect, because the general binding preferences for the amino acids follow the same pattern as for PLP. L-Orn, which has the lowest pK_a among the physiological α-amino acids, is therefore naturally poised to be the best ligand of ODC. However, the binding selectivity of K69R ODC for its physiological ligands (e.g. L-Orn, Put) cannot be explained by the pK_a effect alone. Diaminopropionic acid and diaminobutyric acid have pK_a's lower than for L-Orn, yet K69A ODC preferentially excludes these amino acids from binding, in comparison to their greater reactivity with free PLP. Thus, interactions between the ligand and the enzyme active site provide significant binding energy that favors Schiff base formation with L-Orn over the other tested L-amino acids.

Discrimination for binding of ligands by K69R ODC occurs during Schiff base formation, as reflected by the finding that k_{on} varies with the nature of the ligand, whereas k_{off} is very similar within the diamine or amino acid series. Further, the diamine binding analysis suggests that enzyme selectivity is a function of the binding affinity of the EL′ intermediate. This point is illustrated by the finding that changes in $K_{EL'}$ correlate with the observed differences in the overall K_d's for Schiff base formation, while both k_{+2} and k_{-2} are substantially unaltered within the series (Table 3). In addition, putrescine binds to K69R ODC 24-fold more tightly than L-Orn, and the difference in the binding affinity arises primarily from differences in binding affinity of EL′. Thus, ligand specificity for Schiff base formation with K69R ODC has two probable origins: (1) favorable interactions between the enzyme and the ligand during formation of the Michaelis complex; (2) acceleration of carbinolamine formation from the Michaelis complex through optimal positioning of the amine for reaction with the carbonyl.

Finally, an additional component of ODC substrate specificity is reflected in k_{cat}. The k_{cat} for decarboxylation of L-Orn by wild-type ODC is 4- and 500-fold faster than for L-Lys and L-Arg, respectively. While kinetic binding data for the wild-type ODC are not available, little variation (2−3-fold) in k_{off} is observed for the release of these three amino acids or the products, putrescine and cadaverine, from K69R ODC. Comparison of the carbon-13 isotope effects for decarboxylation of L-Orn and L-Lys by wild-type ODC suggests that decarboxylation occurs more slowly relative to Schiff base decay of the ES species for L-Lys than for L-Orn (*33*). These data suggest that the reductions in k_{cat} for L-Lys and L-Arg are not a reflection of changes in the rates of product release but of slower rates of decarboxylation. Thus, a large component of the substrate specificity in ODC is likely to occur in the transition state for decarboxylation. Similar effects on k_{cat} and on the carbon-13 isotope effects were reported for alternate substrates of arginine decarboxylase (*34*). For ODC, the steps in the reaction that are capable of selectivity are Schiff base formation and decarboxylation, the two steps that are most likely to ensure the fidelity of the reaction. Product release would not provide for overall selectivity in product formation and could not serve as a method to prevent the decarboxylation of inappropriate amino acids within a cell. For PLP-dependent enzymes the rate of bond cleavage is proposed to depend on the precise orientation of the scissile bond parallel to the p-orbitals of the external aldimine bond (*32*). Support for this hypothesis has been obtained through the analysis of the activity of dialkylglycine decarboxylase on series of substrate analogues (*35*) and from structural analysis of an alanine racemase substrate analogue that cannot undergo α-proton abstraction (*36*). Our data suggest that Lys-69 plays a role in the positioning of the CO_2 group for efficient catalysis and that the exact nature of the amino acid side chain is essential to the proper orientation of the CO_2 group, thereby confining catalytic competency to only the biological amino acid, L-Orn.

ACKNOWLEDGMENT

We thank L. Kinch and N. Grishin for helpful discussions.

REFERENCES

1. Tabor, C. W., and Tabor, H. (1984) *Annu. Rev. Biochem. 53*, 749−790.
2. McCann, P. P., and Pegg, A. E. (1992) *Pharm. Therap. 54*, 195−215.
3. Marton, L. J., and Pegg, A. E. (1995) *Annu. Rev. Pharmacol. Toxicol. 35*, 55−91.
4. Wang, C. C. (1995) *Annu. Rev. Pharmacol. Toxicol. 35*, 93−127.
5. Kern, A. D., Oliveira, M. A., Coffino, P., and Hackert, M. (1999) *Structure 7*, 567−581.
6. Grishin, N. V., Phillips, M. A., and Goldsmith, E. J. (1995) *Protein Sci. 4*, 1291−1304.
7. Poulin, R., Lu, L., Ackerman, B., Bey, P., and Pegg, A. E. (1992) *J. Biol. Chem. 267*, 150−158.

8. Toney, M. D., and Kirsch, J. F. (1989) *Science 243*, 1485−1488.
9. Gloss, L. M., and Kirsch, J. F. (1995) *Biochemistry 34*, 3990−3998.
10. Toney, M. D., and Kirsch, J. F., (1993) *Biochemistry 32*, 1471−1479.
11. Nishimura, K., Tanizawa, K., Yoshimura, T., Esaki, N., Futaki, S., Manning, J. M., and Soda, K. (1991) *Biochemistry 30*, 4072−4077.
12. Futaki, S., Ueno, H., Martinez del Pozo, A., Pospischil, M. A., Manning, J. M., Ringe, D., Stoddard, B., Tanizawa, K., Yoshimura, T., and Soda, K. (1990) *J. Biol. Chem. 265*, 22306−22312.
13. Lu, Z., Nagata, S., McPhie, P., and Miles, E. W. (1993) *J. Biol. Chem. 268*, 8727−34.
14. Watababe, A., Kurokawa, Y., Yoshimura, T., Kurihara, T., Soda, K., and Esaki, N. (1999) *J. Biol. Chem. 274*, 4189−4194.
15. Vaaler, G. L., and Snell, E. E. (1989) *Biochemistry 28*, 7306−7313.
16. Coleman, C. S., Stanley, B. A., and Pegg, A. E. (1993) *J. Biol. Chem. 268*, 24572−24579.
17. Tsirka, S., and Coffino, P. (1992) *J. Biol. Chem. 267*, 23057−23062.
18. Brooks, H. B., and Phillips, M. A. (1997) *Biochemistry 36*, 15147−15155.
19. Osterman, A. L., Grishin, N. V., Kinch, L. N., and Phillips, M. A. (1994) *Biochemistry 33*, 13662−13667.
20. Kunkel, T. A. (1985) *Proc. Natl. Acad. Sci. U.S.A. 82*, 488.
21. Grishin, N. V., Osterman, A. L., Goldsmith, E. J., and Phillips, M. A., (1996) *Proteins: Struct., Funct., Genet. 24*, 272−273.
22. Osterman, A. L., Brooks, H. B., Rizo, J., and Phillips, M. A. (1997) *Biochemistry 36*, 4558−4567.
23. Pegg, A. E., and McGill, S. (1979) *Biochim. Biophys. Acta 568*, 416−427.
24. Hiromi, K. (1979) in *Kinetics of Fast Reactions* (Hiromi, K., Ed.) Halsted Press, New York.
25. Morozov, Y. V. Spectroscopic properties, electronic structure, and photochemical behavior of vitamin B6 and analogues. in *Vitamin B6 pyridoxal phosphate* (Dolphin, D., Poulson, R., and Avramovic, O., Eds) pp 325−353, John Wiley & Sons, Inc, New York.
26. Metzler, C. M., Cahill, A., and Metzler, D. E. (1980) *J. Am. Chem. Soc. 102*, 6075−6082.
27. Metzler, C. M., and Metzler, D. E. (1987) *Anal. Biochem 166*, 313−327.
28. Toney, M. D., and Kirsch, J. F. (1991) *J. Biol. Chem. 266*, 23900−23903.
29. Bender, M. L., Begue-Canton, M. L., Blakely, R. L., Brubacher, L. J., Feder, J., Gunter, C. R., Kezdy, F. J., Killheffer, J. V., Marshall, T. H., Miller, C. G., Roeske, R. W., and Stoops, J. K. (1966) *J. Am. Chem. Soc. 88*, 5890−5912.
30. Osterman, A., Kinch, L. N., Grishin, N. V., and Phillips, M. A. (1995) *J. Biol. Chem. 270*, 11797−11802.
31. Leussing, D. L. (1986) Model Reactions. in *Coenzymes and cofactors: vitamin B6 pyridoxal phosphate, chemical, biochemical and medical aspects* (Dolphin, D., Poulson, R., and Avramovic, O. Eds.) pp 102−112, John Wiley & Sons, New York.
32. Dunathan, H. C. (1966) *Proc. Natl. Acad. Sci. U.S.A. 55*, 712−716.
33. Swanson, T., Brooks, H. B., Osterman, A. L., O'Leary, M., and Phillips, M. A. (1998) *Biochemistry 37*, 14943−14947.
34. O'Leary, M. H., and Piazza, G. J. (1981) *Biochemistry 20*, 2743−2748.
35. Sun, S., Zabinski, R. F., and Toney, M. D. (1998) *Biochemistry 37*, 3865−3875.
36. Stamper, C. G. F., Morollo, A. A., and Ringe, D. (1998) *Biochemistry 37*, 10438−10445.
37. Fasman, G. D. (1976) in *Handbook of Biochemistry and Molecular Biology. Physical and Chemical Data* (Fasman, G., Ed.) 3rd ed., Vol. I., CRC Press, Cleveland, OH.

BI9906221